Biotribology 35–36 (2023) 100263

Contents lists available at ScienceDirect

Biotribology

journal homepage: www.elsevier.com/locate/biotri

Tribo-Mechanical Properties and Bioactivity of Additively Manufactured PAEK Materials for Load Bearing Medical Applications: A Systematic Review

Benjamin A. Clegg, Dilesh Raj Shrestha, Nazanin Emami *

Polymer-tribology and Biotribology group, Division of Machine Element, Luleå University of Technology, Sweden

ARTICLE INFO

Keywords:
PEEK
3D printing
Additive manufacturing
Tribology
Medical
Bioactivity

ABSTRACT

Additive manufacturing (AM) holds significant potential in transforming medical applications, with a particular focus on polyetheretherketone (PEEK) and its derivatives, collectively known as poly-aryl-ether-ketone (PAEK) materials. Advances in AM precision have paved the way for the successful 3D printing of high-performance thermoplastics like PEEK, offering new prospects in load-bearing medical applications. This systematic review comprehensively assesses recent scientific literature concerning the tribo-mechanical properties and bioactivity of additively manufactured PAEK materials, with a specific emphasis on PEEK, for load-bearing medical uses. Despite substantial research into AM of metallic biomaterials, knowledge gaps persist regarding AM processing parameters, structure-property relationships, biological behaviours, and implantation suitability of PAEKs. This review bridges these gaps by analysing existing literature on the tribo-mechanical properties and bioactivity of additively manufactured PAEK materials, providing valuable insights into their performance in load-bearing medical applications. Key aspects explored include printing conditions, strength limitations, and outcomes of in-vitro and in-vivo evaluations. Through this systematic review, we consolidate current knowledge, delivering essential information for researchers, clinicians, and manufacturers involved in advancing additively manufactured PAEK materials for load-bearing medical applications.

1. Introduction

Load-bearing medical applications, such as orthopaedic implants, require materials that possess exceptional mechanical properties, biocompatibility, and the ability to promote successful integration with the surrounding tissues [1]. In recent years, polyetheretherketone (PEEK) and its derivatives have emerged as promising candidates for these applications due to their outstanding combination of properties. Additionally, the advent of Additive Manufacturing (AM), or 3D printing, has further enhanced the potential of PEEK-based materials by enabling the fabrication of complex geometries with tailored material properties [2–4].

PEEK is a high-performance thermoplastic polymer that exhibits excellent mechanical strength, thermal properties, resistance to wear and fatigue, and biocompatibility [1,5]. It is utilised in load-bearing medical applications [6], including spinal implants [7], joint replacements [8], and dental prosthetics [9]. PEEK's similarity to bone in terms of mechanical properties (avoiding the stress shielding effect [10]), coupled with its radiolucency and resistance to corrosion, has made it an attractive alternative to traditional metallic implants [1].

Additive manufacturing (AM) has revolutionized the fabrication of medical devices by enabling the production of complex structures with

Abbreviation: PAEK, PolyArylEtherKetone; PEEK, PolyEtherEtherKetone; PEKK, PolyEtherKetoneKetone; PLA, Polylactic Acid; PVDF, Polyvinylidene Fluoride; PMMA, Poly(methyl methacrylate); PP, Polypropylene; PETG, Polyethylene Terephthalate Glycol; Tg, Glass Transition Temperature; XRD, Xray Diffraction; CoF, Coefficient of Friction; Mg^{2+}, Magnesium Ions; PAA, Polyacrylic Acid; EDA, Ethylenediamine; ALP, Alkaline Phosphate; HT-LS:, High Temperature Laser Sintering; FDM, Fused Deposition Modelling; FFF, Fused Filament Fabrication; AM, Additive Manufacturing; PBF, Powder Bed Fusion; HT-LPBF:, High Temperature - Laser Powder Bed Fusion; LPBF, Laser Powder Bed Fusion; SLS, Selective Laser Sintering; HAp, Hydroxy Apatite; ZnHAp:, Zinc doped Hydroxy Apatite; cHAp, Calcium Hydroxy Apatite; CF, Carbon Fibre; CFR, Carbon Fibre Reinforced; GNP, Graphene Nano-Platelets; CNT, Carbon Nano-Tubes; AKM, Akermanite; AMP, Amorphous Magnesium Phosphate; rGO, Reduced Graphene Oxide.

* Corresponding author.
E-mail address: nazanin.emami@ltu.se (N. Emami).

https://doi.org/10.1016/j.biotri.2023.100263
Received 3 August 2023; Received in revised form 1 November 2023; Accepted 2 November 2023
Available online 5 November 2023

high precision [11]. This technology enables customization of implants based on patient-specific anatomical data, leading to improved fit and functionality [12]. AM also offers the potential to incorporate porosity [13,14] and surface modifications [15–17], enhancing the bioactivity and osseointegration of PEEK materials [1]. However, questions remain regarding the long-term viability of these materials, as most existing studies only provide short-term testing [1].

The development of computer tomography (CT) and magnetic resonance imaging (MRI) has helped to convert the models easily into 3D models. These models can be sliced using slicing software that can read by the 3D printers. Once the design is prepared, the printer can independently execute the printing process according to the design. The 3D printing process typically involves three fundamental steps:

Step 1: 3D model design and convert to Standard Tessellation Language (.STL) format.

Step 2: Slice the design using slicing software and send to the 3D machine.

Step 3: Print the component layer by layer as sliced in the slicing software.

There are 7 categories of 3D printing methods described by American Society for Testing and Materials (ASTM) 52,900:2021 [18]. This report focus' on Fused filament fabrication (FFF), commonly known as fused deposition modelling (FDM), after it was introduced and commercialised by Stratasys Company.

In FFF, neat polymer or polymeric based materials are extruded from the extruder head and deposited layer by layer to create the final product, which then solidifies into the desired shape. Key elements in the FFF printing method include print head size, cooling, material feed mechanism, build surface, build temperature, bead width, air gap, and raster orientation [19]. Adjusting these parameters allows control over the quality of the printed parts orientation [19,20]. In powder bed fusion, the powder is loaded into the powder container of printing machine equipped with the laser. The slicing process is similar to that of an FFF printer, although different parameters are set due to the involvement of the laser such as the intensity of the laser, scan speed and scan space along with the bed temperature, layer thickness. The printing process is conducted in an inert atmosphere, and after achieving the desired shape and size, the non-sintered powder is collected and can be reused.

While the advantages of additively manufactured PEEK materials such as patient specific implants, and complex designs for load-bearing medical applications are evident, there remain numerous challenges related to the processing, accuracy, and performance of 3D printed polymers [21,22]. The tribo-mechanical properties encompass mechanical strength, wear and frictional behaviour, fracture toughness and fatigue resistance, which directly influence the longevity and performance of load-bearing implants, such as hip and knee tribological configurations. Moreover, the bioactivity of these materials refers to their capacity to interact with living tissues, promote cell adhesion, proliferation, and facilitate the regeneration of bone tissue.

The primary objective of this review is to assess the mechanical properties of additively manufactured PEEK materials, including processability and printability of PEEK and PEEK based materials. Additionally, the tribological behaviour of these materials, such as wear resistance and frictional characteristics, will be thoroughly examined to comprehend their performance under real-world load-bearing conditions. Furthermore, the bioactivity of additively manufactured PEEK materials will be a key focus of this review. Understanding their ability to promote cell adhesion, proliferation, and osseointegration is crucial for successful clinical implementation [1]. The findings of this systematic review will have significant implications for researchers, clinicians, and biomedical engineers involved in the development and application of load-bearing medical devices.

In the subsequent sections of this review, the authors will explore the methodologies employed, summarize the results obtained, and discuss the implications of the findings for the field of load-bearing medical applications. By synthesizing the current body of knowledge, this systematic review aims to contribute to the advancement of additively manufactured PEEK materials and their translation into clinical practice.

2. Methods

The research question for this systematic review is: "What are the tribo-mechanical properties and bioactivity of additively manufactured PAEK materials used in load bearing medical applications?" The literature search was conducted using the following databases: PubMed, SCOPUS, and Web of Science. The search terms and keywords are:

1. ("PEEK" OR "paek" OR "pekk" OR "pekkek" OR "polyetheretherketone") AND ("additive manufacturing" OR "three-dimensional printing" OR "3D printing")
2. ("medical" OR "biomedical" OR "orthopaedic" OR "implant" OR "total joint replacement" OR "arthroplasty" OR "joint replacement")
3. ("tribology" OR "friction" OR "wear" OR "lubrication") AND ("medical" OR "medicine" OR "biomedical" OR "orthopaedic" OR "implant")
4. ("PEEK" OR "polyetheretherketone" OR "PEKK" OR "polyetherketoneketone" OR "PAEK" OR "Polyaryletherketone") AND ("medical" OR "biomedical") AND ("3D printing" OR "additive manufacturing" OR "three dimensional printing") AND ("Bio* Response") AND PUBYEAR >2020

For Mechanical search: 1 and 2.
For Tribological search: 1 and 3.
For Biological activity search: 4.

The search was limited to relevant studies published up to the knowledge period from 2010 to early 2023. Search 1 aims to cover a wide range of studies, used as a broad search to initialise the review. Search 1 was then used in conjunction with 2&3 to cover a wide range of papers to assess. For the biological section, the review was restricted to 2020 due to a previous review [23] comprehensively addressing this period of time.

Language restrictions to English were applied.

2.1. Study Selection

Initially, two searches were conducted (Search 1&2) which yielded 345 papers, another search (Search 1&3) resulted in 31 papers, and a third search (Search 4) provided 38 papers. After eliminating duplicates, the authors were left with a pool of 654 studies for screening. Out of these, 579 studies were excluded based on factors such as relevance to the research question, study design, and outcome measures. Ultimately, we included 75 studies in this review.

Excluded papers were Non-English, studies off topic, PEEK not 3D printed, not medical and not a PEEK material.

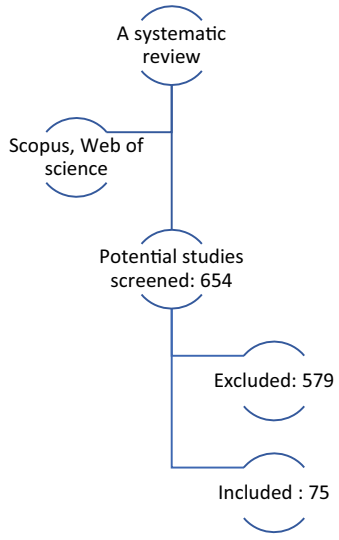

2.2. Data Extraction

Data extraction was performed separately for each section (mechanical, tribological, and bioactivity). The variables of interest included specific tribo-mechanical properties (e.g., wear resistance, mechanisms of wear, friction coefficient, mechanical strength, fracture behaviour, compressive and tensile properties, and bioactivity measures (e.g., osseointegration, cell adhesion, biocompatibility). Standardized data extraction forms were used to ensure consistency.

The authors extracted data from each included study. Discrepancies were resolved through consensus. The quality and risk of bias of the included studies were assessed separately for each section. Appropriate quality assessment tools were used, such as the PRISMA guidelines and domain-specific tools if available. Due to the heterogeneity of the included studies, a narrative synthesis was conducted for each section.

The findings from the mechanical, tribological, and bioactivity sections were summarized separately. No meta-analysis was performed.

The systematic review followed the PRISMA guidelines. A flow diagram was created to illustrate the study selection process. The included studies in each section (mechanical, tribological, and bioactivity) were summarized in detail, including study characteristics, methodology, and key findings. The findings were presented in a clear and organized manner, addressing the research question.

2.3. Limitations

Potential limitations of the systematic review include the exclusion of unpublished studies, potential publication bias, and the possibility of missing relevant studies due to the search strategy and language restrictions.

2.4. Method Overview

The systematic review provides insights into the tribo-mechanical properties and bioactivity of additively manufactured PAEK materials for load bearing medical applications. The findings highlight the current state of knowledge in this field and identify gaps for future research.

3. Tribo-Mechanical Properties

3.1. Neat PAEK Material

3.1.1. Printing Parameters

Incorrect heat distribution during printing could cause warpage and delamination and as such it must be managed throughout the printing process [14]. Specifically, the extrusion temperature and head design along with ambient temperature to create a successful print. Inadequate heat distribution during the printing process can impact the material's crystallinity and internal structural flaws, resulting in compromised mechanical properties.

Different researchers have utilised various parameters to improve the printing quality, outlined in APPENDIX A: 3D printing of Neat PAEK.

Print speed and temperature, layer thickness and filling ratio all influence the tensile properties of FFF PEEK [24]. The improvement in tensile properties is attributed to the improved fusion effects and interlayer bonding. Wang et al. [25] investigated tensile strength alongside surface quality and microstructure, finding that to reduce internal defects and increase layer bonding strength a higher print temperature alongside a lower print speed and layer height was required. With this the optimised parameters of 440 °C nozzle temperature, 20 mm/s print speed and 0.1 mm layer height were determined. Similar investigations were carried out by [26,27] for PEEK and [28] for PEKK.

Build orientation was optimised using PEEK cranial implants on a HT-LS printer [29]. The various building orientation and raster angles are shown in Fig. 1. The inverted horizontal and horizontal orientations were optimum for compressive strength and minimal design deviation, echoed by Arif et al. [30], who also added that a 0° raster angle was optimum for tensile, flexural as well as fracture toughness properties. This can be ascribed to each configuration having various thermal gradients between the beads, leading to a differing degree of interfacial adhesion. Vindokurov et al. [31] demonstrated an optimised tensile and elasticity properties with an infill angle 180° followed by 90° and 45°. Similarly, a raster angle of 30° with horizontal orientation was shown to be preferred when optimizing mechanical properties, although it is still inferior to injection moulded PEEK [32]. It should be noted that the raster angle has been shown not to affect the microstructure of thermal properties of the polymer, but it does affect the bulk crystallinity [32]. However, others [28,33] have suggested that crystallinity is not affected by printing parameters. This could be due to the multitude of factors affecting the polymer material as it is processed.

Voids and defects produced by manufacturing within the material are usually present at the wall and infill junction [34], these act as stress concentration sites and can initiate cracks which eventually propagate, and result in fracture and material/component failure. To decrease these internal defects, it is suggested that the infill density should be increased, and inner wall and infill travel paths should be decreased.

3.1.2. Thermal Management

Without correct thermal management, anisotropy within the material of different zones of crystallinity can be seen during the printing process [12]. To counteract this, Qu et al. [35] varied the ambient and substrate temperatures, with optimal mechanical properties determined to be at higher ambient (90 °C) and substrate temperatures (160 °C). Optimisation of nozzle, chamber and bed temperatures were also carried out [36]. These parameters ensure enhanced interlayer bonding, due to the reduced cooling of the material, with temperatures nearer to the Tg.

Due to the high melting temperatures required to print PEEK (above 380 °C), the material undergoes large temperature changes as the material is extruded, which could lead to warpage, internal stresses, and delamination. Hu et al. [37] designed an augmented nozzle with a heat collector to ensure uniform printing area temperature, decreasing warpage from 20.4% to 5%, alongside enhanced interlayer bonding and crystallinity resulting in an elastic modulus increase of 20%.

An effective novel approach, that incorporated high printing temperature and plane printing, was taken by Tseng et al. [38] to print PEEK using a screw extrusion method. Achieving a homogenously layered part with a 96% bulk material strength.

3.1.3. Annealing

Annealing is a common post-processing technique used for PEEK (polyetheretherketone) to increase its crystallinity, which can impact the mechanical properties of semi-crystalline polymers. It has been found that increasing the crystallinity through annealing can lead to higher yield strength but a lower toughness in PEEK [39]. The post-processing technique of annealing can aid the relief of internal stresses introduced during fabrication, leading to enhanced interlayer adhesion and increased crystallinity. However, it is significantly more effective at slower printing speeds (1500 mm/min compared to 2000 mm/min) [39], resulting in a 14% increase in compression strength for slow speeds, as opposed to an insignificant increase for high-speed printing.

The annealing process has been shown to result in a significant enhancement of tensile strength, with improvements of up to 28% [31,40], and an increase in crystallinity and flexural modulus can be observed [41]. The annealing process changes the structure of pores while there are contradictions on whether the annealing process alters the overall porosity, with [39] stating no change but [33] stating a decrease. The discrepancy [33,39] could be attributed to the annealing process compounding pores into larger pores around stress points, but this can be highly dependent on the printing conditions, annealing temperature, and the pore locations.

Overall, the effects of annealing can be observed to increase the

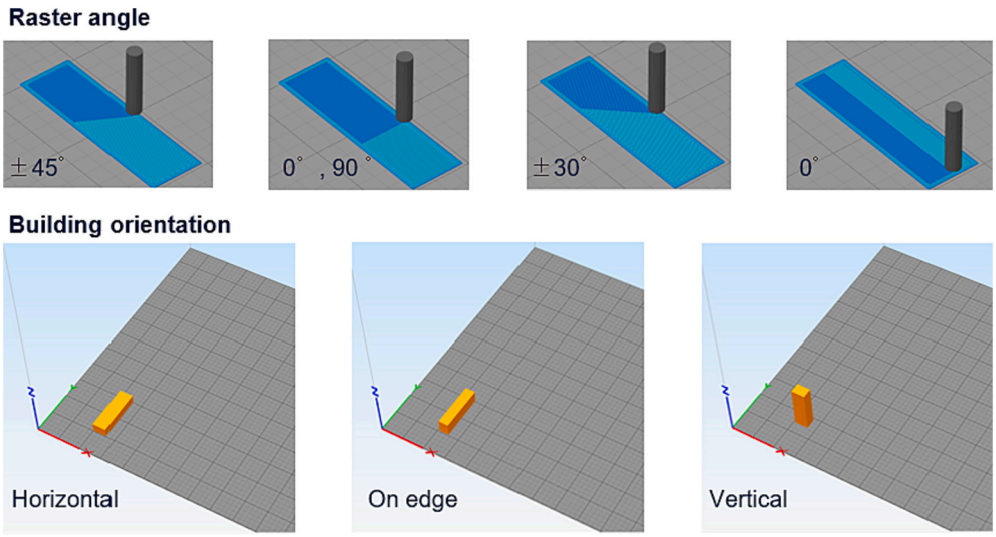

Fig. 1. Raster angle and build orientation in 3D printing FFF.

mechanical properties of the bulk polymer. However, when considering the interlayer bonding, this should be enhanced via optimisation of the printing parameters.

3.1.4. Nozzle

The most influential parameter for increasing printing accuracy is that of the nozzle diameter as discussed by Wang et al. [42]. Followed by an increased nozzle temperature (400–440 °C) [40–42], slower printing speeds (15–50 mm/s) [41,42], and a reduced layer height (0.1–0.2 mm) [41]. These parameters allow for the production of consolidated and more dense materials with increased mechanical strength and a reduction of internal defects [41,43].

The effect of wait time (pausing), between printed layers, (11–25 s), on interlayer bonding is also significant [41]. If the wait time is increased, the previous printed layer will cool to the ambient temperature at a higher rate than if another layer was applied, allowing a shorter time for the polymer chains to align and form crystalline structures. It should however be noted that these parameters are all related, and various combinations may result in different optimisations. For example, layer height being the most influential for modulus control and the flexural stress determined via nozzle temperature [41].

3.1.5. Porous Scaffolds

Neat PEEK is known to be biologically inert [1]. To counteract this, porous scaffolds within the bulk matrix have been developed (Fig. 2), increasing the effect of bone ingrowth, further detail on the biological aspect will be described in Biological activity section. However, with increasing porosity comes a decrease in mechanical properties.

Feng et al. [44] demonstrated a decrease in compressive Young's modulus and strength with pore size from 300 to 600 μm. Studies also analysed the effect of pore design using FFF [45] and PBF [46], with both studies confirming that a diamond porous design provided the highest elastic modulus.

For FFF printed parts [45], the variance of pore size from the selected 600 μm, was the highest in gyroid design and most consistent in rectilinear. It should be noted that a variance in pore size may be preferrable for enhanced biological activity, (more in Biological activity). For PBF [46] it was determined that the optimal pore shape was gyroid with benefits of ease of processing, precision, mechanical properties, and low volume fracture deviation.

Even with improving technologies, it is known that AM thermoplastic components still lack equal mechanical performance to that of their machined counterparts [47]. With 3D printed parts showing lower tensile (76.5%) and flexural strength and fracture toughness, although higher in micro hardness [16]. This can be ascribed to anisotropy within the additive material, leading to a higher probability of surface defects, thereby increasing the likelihood of failure [47]. This leads the review to the benefits of PAEK and its composites.

3.2. PAEK Composites

Various methods to improve the mechanical integrity of the polymer material whilst simultaneously enhancing the bioactivity, have been undertaken (see APPENDIX B: PAEK 3D printed composites). The 3D printing of polymer composites with nanoparticles presents significant challenges. Achieving uniform dispersion of nanoparticles within the polymer matrix is difficult due to agglomeration and poor interfacial adhesion, which can lead to inconsistent material properties [48].

Printability issues, including nozzle clogging, can arise from changes in the polymer's rheological behaviour caused by nanoparticles [49–54]. Moreover, high nanoparticle loading, often necessary for improved performance, can increase material costs and exacerbate dispersion challenges [54]. Addressing these issues requires careful material selection, surface modifications, and process optimization to ensure successful and cost-effective 3D printing of high-quality polymer nanocomposites. Ranging from the incorporation of HAp [48,55,56], Carbonaceous based reinforcements [49–54], novel combinations [57–59] and coatings [60–62]. To validate these composites and predict their behaviour, computational methods were utilised [55,59,63].

3.2.1. Hydroxy Apatite (HAp)

PEEK scaffolds with HAp were FFF fabricated [55] with a uniform distribution, leading to an increase in crystallinity from 19.8% up to 28.7% for neat PEEK and a PEEK/HAp content of 40 wt% respectively, reported by [56] using XRD. This increase in crystallinity is due to the HAp particles acting as the heterogeneous crystallization nucleation points, however, this results in reduction in elongation to break and toughness [55].

The addition of HAp and porous scaffolds allows for a greater range of tuneable mechanical properties, by varying the pore size from 2.0 to 0.2 mm, an increase in Young's modulus 50.6 - 624.7 MPa and strength 2.2 - 35.2 MPa can be achieved [55].

Rodzen et al. [48] demonstrated the possibility to manufacture up to 30 wt% HAp in PEEK, but beyond this agglomeration becomes more prominent. The authors [56] later demonstrated that the inclusion of HAp results in an increase of crystallinity in both the bulk and the surface region of the composite. This benefits the bioactivity and the mechanical performance of the material with the need for post processing.

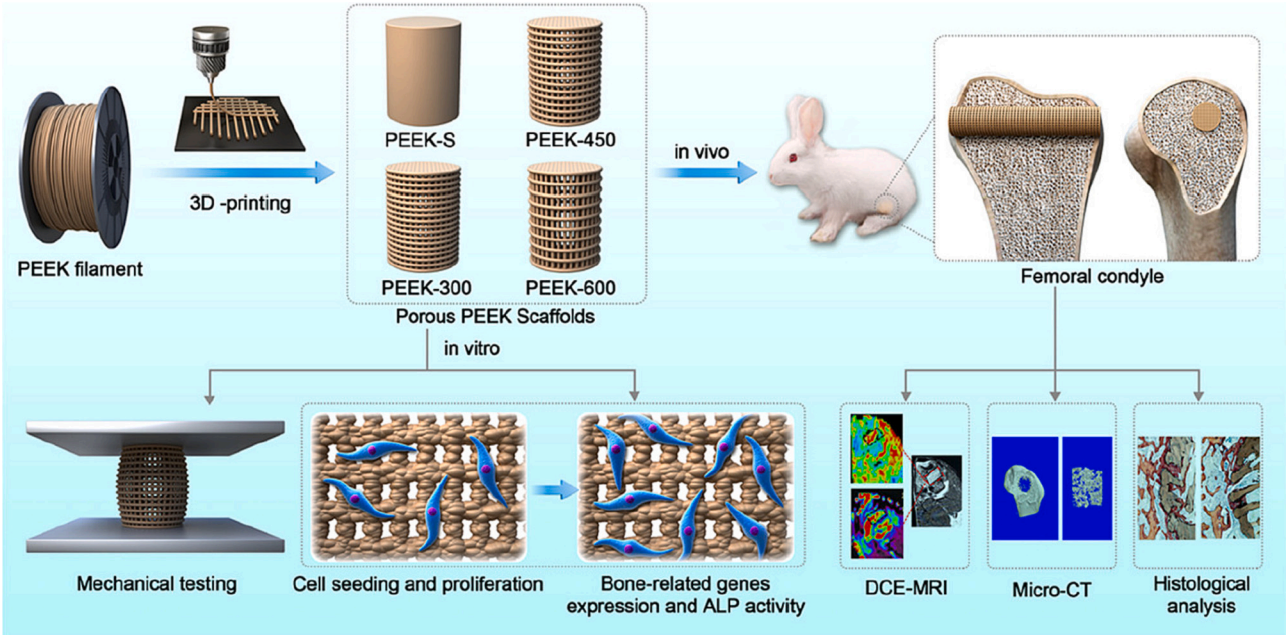

Fig. 2. Illustrative representation showcasing the fabrication process of porous PEEK scaffolds, highlighting their intended use in various biological applications [44] [Reprinted with permission from ACS. https://pubs.acs.org/doi/10.1021/acsomega.0c03489].

Manzoor et al. [64–66] investigated how strontium and zinc doped HAp would affect the performance of PEEK via FFF. A non-significant reduction in mechanical properties was seen from both pure and doped composites [65] when compared to neat PEEK. This can be attributed to the poor adhesion between the particles and matrix materials.

3.2.2. Carbon Fibre

The incorporation of carbon fibre to the PEEK matrix improved many aspects of mechanical properties including tensile, bending, and compressive strengths compared to injection moulded neat PEEK [49]. Li et al. [54] discovered that the addition of short carbon fibres can increase the uniformity of the nucleation whilst decreasing layer bond strength, thereby increasing the porosity due to the change in fracture mode. Both [54,67] concluded that the optimal printing orientation for bonding quality and mechanical performance was vertical printing, for CF PEEK and PEEK CFR sandwich structures in FFF.

Efforts have been made to increase the quality of material produced [53,68]. Using FFF, the proposed parameters [53] of a raster angle of ±45° and smaller layer thickness (~0.1 mm) can lead to a better surface quality and reduced number of defects within the bulk, and a custom nozzle system with a smoother inner surface allows for variable outlet angles [68], resulting in reduced fibre damage/less shortening of the fibres. The effect on the exact fibre orientation is inconclusive, but overall, the uninterrupted nozzle flow should allow for an increased quality of AM printed composite.

A soluble support material (styrene-acrylic copolymer) has been developed by Santiago et al. [63] for use in 3D printing of high temperature PEEK, CF PEEK and PEKK. Thereby, creating a part with accurate and defined dimensions whilst successfully removing defects from the material, due to overhangs.

3.2.3. Carbon Nanomaterials

Both [50,51] investigated the effects of GNP and CNT within a PEEK matrix. Notably the coefficient of thermal expansion was decreased, by 26% and 18% using 5 wt% GNP and 3 wt% CNT respectively, allowing for increased dimensional stability. A uniform distribution of the reinforcements enhanced the storage modulus in the glassy region of the samples. A variation in fracture modes is exhibited with CNT composites showing brittle fracture and GNP composites displaying ductile fracture, compared with neat PEEK. The authors attribute this to the lower Poisson's ratio of the GNP composite with a greater extent of micro voids compared to the CNT composite and neat PEEK [50]. Alam et al. [51] also included the process of sulfonication to increase bioactivity, stating that any mechanical loss incorporated was recovered via the use of nanoparticle reinforcements.

A 1 wt% GNP/PEEK filament with excellent thermal stability and improvement in storage modulus, tensile strength, Young's modulus and elongation to break 61%, 34%, 25% and 37% respectively compared to neat PEEK was developed by Yaragalla et al. [52]. The author attributes the success to the uniform dispersion alongside a strong interface via hydrogen bonding of the matrix and reinforcement.

However, as the weight percentage of graphene nanoplatelets (GNPs) surpassed 1 wt%, a shift towards a more brittle fracture mode was observed, which was attributed to the agglomeration of GNP layers [52], suggesting that agglomerates acted as stress concentration sites within the PEEK matrix. Contrastingly, Arif et al. [50] does not report any brittle fracture behaviour with increase in GNP content. This variance in results can be attributed to the studies focusing on different stages within the materials manufacturing process: one study analysed the filament [52] and the other examine the material after printing [50].

3.2.4. Novel Approaches

Recently innovative strategies have been explored to simultaneously maintain mechanical performance whilst increasing biological activity. Such as: PEEK/AKM composites [69] that are able to match the cancellous bone properties, via HT-LPBF; PEEK/AMP blends that enhance processibility [58] and mechanical performance [69]; and a highly tuneable bio glass 45S5 powder (45 wt% SiO_2, 6 wt% P_2O_5, 24.5 wt% Na_2O, and 24.5 wt% CaO) PEEK composite using LPBF, with enhanced processability vs neat PEEK due to increased thermal conductivity [70]. Also, a successful attempt to increase the interlayer strength (130%) and reduce anisotropy (to 1.1%), amorphous PAEK was used as an interlayer reinforcement [71].

3.2.5. Coatings

The utilisation of coatings has been explored, with improvements in biological activity due to increases in wettability [60] using a 500 nm Ti

coating, with no phase changes in either PEEK or Ti during sputtering. cHAp and rGO have also been studied as surface coatings by Oladapo et al. [61,62], successfully improving the biological properties and simultaneously improving Young's and bulk modulus versus neat PEEK.

Taking all of this into account, there remains an issue associated with the presence of voids and porosities, which are typical characteristics resulting from the material deposition process in Fused Filament Fabrication (FFF) [32]. These voids and porosities affect the performance disparity between conventionally manufactured solid materials and 3D-printed bulk samples [14]. A higher volume of voids has been observed to correlate with reduced Ultimate Tensile Strength (UTS), as exemplified by the case of PEEK 3D-printed lumbar cages, which could only support up to 63% of the ultimate load compared to their injection-moulded counterparts [7]. To enhance the performance of 3D-printed PEEK materials, various researchers have endeavoured to optimise different printing parameters, as discussed earlier, with the aim of minimising the gap between conventionally manufactured PEEK and 3D-printed variants. Additionally, there has been a growing interest in reinforcing these materials, as several studies have demonstrated the potential to enhance the strength and stiffness of printed samples through the incorporation of reinforcements.

3.3. Tribological Performance

PEEK possesses several advantageous bulk properties, including radiolucency, high strength and mechanical properties as previously discussed along with good wear resistance [1]. These characteristics make it a promising candidate for orthopaedic biomaterials.

Arif et al. [50] performed a fretting wear test, investigating the tribological performance of the CNT and GNP reinforced PEEK via FFF. It was shown that the CoF was reduced via the addition of nanomaterials. However, a higher wear rate was seen, Table 1. The factors ascribed with the increase in wear and reduction in friction are: a decrease in bulk hardness; density; and an increase in the multiscale porosity of the composite samples.

Gonçalves et al. [72] incorporated the use of CNT and GNP/PEEK via FFF. Stating a 60% reduction in CoF with 3 wt% GNP, due to the self-lubricating effect, but large voids were measured in the production. Similarly, Golbang et al. [73] investigated PEEK/(IF-WS2). With notable levels of dispersion and interaction with PEEK matrix, helped by low tendency for agglomeration, paired with low shear rates during AM due to shear thinning behaviour. Additionally, the nanoparticles reduced wear and friction of PEEK nanocomposites compared to pure PEEK. Yang et al. [74], were able to enhance the friction and wear resistance of PEEK using 0.5 wt% f-GO. With a reduction of CoF 27.3% and specific wear rate of 18.3%. The functionalization of the GO allowed for an increased interfacial adhesion, allowing a smaller wt% than GO thereby preventing any reduction in toughness.

3.3.1. PEEK as a Substrate for Coating

In a study by Cvrček et al. [75], the CoF and wear track width of various TiNb coatings of 3D PEEK were evaluated. The TiNb coated 3D PEEK showed a similar CoF to 3D printed PEEK, while the anodic oxidation treated 3D PEEK had a slightly higher CoF and the highest wear track width, all showing satisfactory adhesion. The primary wear mechanism for TiNb coated 3D PEEK was adhesive, while for anodic oxidation treated 3D PEEK, it was abrasive. In the case of 3D printed PEEK, both adhesive and abrasive mechanisms were observed.

Table 1
CoF and wear rate of PEEK and PEEK composites [72].

Material	CoF	Wear rate (mm^3/Nm)	Vickers hardness H_V
Neat PEEK	0.25	1.23	302
1 wt% CNT/PEEK	0.08	2.97	238
3 wt% GNP/PEEK	0.10	2.72	279

In summary, there is a distinct lack of studies investigating the tribological behaviour of 3D printed PAEKs in load-bearing orthopaedic applications, using correct tribological configurations, resulting in limited clinical application and relevant tribological setups. Existing studies cover a range of applications, including dental implants [73] in micro abrasion setups and dry sliding setups. The studies of [50,73–75] were dominated by abrasive wear and only assessed over short time periods. Specifically [50], utilised dry fretting, which is associated with adhesive wear dominance [76]. Moreover, the current studies only provide short-term testing, while longer-term testing is needed to assess the material's long-term viability in tribological and orthopaedic applications. Notably, none of the studies incorporate a biologically representative lubricant such as FBS, which is crucial for clinically relevant tribological systems. Both the mechanisms of adhesive and abrasive wear alongside the frictional behaviour, should be studied within a relevant biological system, to gain a comprehensive understanding of the tribological behaviour of AM PEEK in orthopaedic applications.

3.3.2. Guide to Readers about Wear Particles

A review cast in 2016 by Stratton-Powell et al. [77] outlined studies investigating PEEK-based particles produced by joint replacement simulators, the mean particle size ranged from 0.23 μm to 2.0 μm, with an absolute range of approximately 0.01 μm to 50 μm. Histologic analysis of human tissue identified rod-like carbon particulates and granular-shaped PEEK particles. Multiple studies examined the biological response to PEEK-based particles, including animal models, cell line experiments, and human tissue retrieval studies. In animal studies, immunologic cell infiltration was similar between PEEK and UHMWPE particles. However, one in-vitro study showed increased inflammatory cytokine release, and only one study tested the effects of particle size on cytotoxicity, finding toxic effects for larger unfilled PEEK particles. Overall, PEEK-based wear particles were mostly in the phagocytozable size range. Improvements are needed in preclinical testing, including human tissue retrieval studies and in-vitro cell studies using isolated wear particles or validated joint replacement simulators.

However, the authors were unable to discover studies specifically examining the wear particles of 3D printed PEEK, which could lead to variations in the wear particles generated by the tribological system, potentially eliciting different responses from the local biological environment. The layered structure deposited through the 3D printing process introduces voids, interfaces, and varying levels of interlayer bonding [34,36,37,72], which may impact wear mechanisms in a biotribological system. Additionally, the surface roughness [16,17] of 3D printed PEEK can contribute to the production of wear particles with irregular sizes and shapes compared to smoother conventionally manufactured parts.

Furthermore, the presence of reinforcements like carbon fibres or nanoparticles in 3D printed PEEK can serve as nucleation sites for crystallization [54,55], and their distribution and orientation may significantly affect the morphology of the wear particles.

It is important to note that a decrease in wear does not directly correlate with a decrease in the biological activity of wear particles [78]. Consequently, thorough investigation of the biological impact of wear particles from AM-manufactured materials should be conducted before clinical progression.

4. Biological Activity

Biological activity refers to the ability of a material to interact with living tissues in a way that promotes positive biological responses. This includes the material's capacity to support cell viability, encourage cell adhesion, and facilitate osteoblast differentiation [1]. In the context of biological implants, these properties are essential for successful tissue integration and regeneration, leading to improved overall biocompatibility and clinical outcomes.

This section will provide an overview of implemented techniques resulting in modifications and changes in surface characteristics of the component. The effect of the modifications on cell adhesion, proliferation, differentiation, and mineralisation, as well as mechanical properties and antibacterial activity, is summarized in Table 2. By synthesizing the results of these studies, this study hopes to provide insights into the potential of surface modification techniques to enhance the performance of 3D-printed PEEK implants and ultimately improve patient outcomes. The authors would like to refer readers to a prior comprehensive review by Basgul et al. [23] that provides an overview of significant advancements in the field of additive manufacturing (AM) utilizing polyaryletherketones (PAEKs) up until 2020.

4.1. Composites

Eight, studies [55,56,64,65,79–82], examined how the addition of hydroxyapatite HAp to the PEEK matrix can enhance the bioactivity of the sample. Both Rodzen et al. [56] and Zheng et al. [55,82], demonstrated that a FFF printing process can be used to create a biologically active surface with a PEEK/HAp porous composite. With increasing apatite (mineral essential for bone development in-vivo) formation on the surface with increasing wt% of HAp. But with Zheng et al. [55] suggesting that the increase in formation is an indirect effect of the addition of HAp, which increases surface area and roughness, thereby increasing cell proliferation and mineralisation.

Manzoor et al. [65] explored the effects of doped HAp composites, to target and enhance specific responses. Strontium for osteoblast proliferation and Zinc for antimicrobial properties, later developing this further craniomaxillofacial implants [66]. Demonstrating that these compounds can be suitably manufactured for an FFF printing process whilst achieving high levels of bioactivity. Manzoor et al. [64] then later developed a ZnHAp composite that has improved bioactivity but does not study the effects of bacteria inhibition.

The positive bioactive effect of adding cHAp was examined and confirmed by Oladapo et al. [62,79] who also explores a rGO/cHAp coating [61]. The addition of HAp via an AMX nanocoating was also explored by Hu et al. [80], creating a material with an antibacterial and hydrophilic surface leading to 11% against <1% cell coverage for neat PEEK. A TiNb coating was also explored [75] with a significant increase in bioactivity.

Amorphous magnesium phosphate (AMP) particles blended with PEEK, were investigated [58], for the potential positive influence of Mg^{2+} ions on cellular activities and confirmed. A key suggestion was noted that a stable interfacial layer is key for enhanced osteointegration.

Carbon reinforcements such as FFF PEEK-CFR can also create a hydrophilic surface and at 5% can improve mechanical performance [49]. With 3D printed surfaces outperforming polished and sandblasted processes, via increased surface areas. Alam et al. [51] showed CNTs and GNPs can improve apatite formation, but only with help of sulfonication.

A multi material SLS approach for PEEK/β-TCP allowed host bone connection in the defected region at 8 weeks post implant [83]. This process deployed biodegradable PLLA, that vacates and allows body fluid exchange with the implanted β-TCP. A bespoke process [81] of 3D printed HAp scaffold with PEEK compression moulded over it, was also biologically and mechanically successful. Gao et al. [84], designed a PEK-CN/nHAp compound to overcome the limits of PEEK/nHAp crystal lattices, whilst maintaining the consistent, and closer mechanical properties with cortical bone than neat PEEK. Gao et al. [85,86] later discovered a novel approach to low temperature printing of PAEK-COOH bioinks, with promising results in-vitro & vivo.

In conclusion, the studies reviewed indicate that the addition of hydroxyapatite (HAp) to the PEEK matrix can enhance the bioactivity of the material, leading to increased surface apatite formation, improved cell adhesion, and potential for bone tissue repair. The optimal percentage of HAp varies between studies, with some showing improved properties at 10 wt%, while others suggest higher levels such as 15 wt% or 30 wt%. The studies also suggest that other additives, such as Zinc [64], and AKM [69], can be incorporated into the PEEK matrix to enhance its properties. Further research is needed to investigate the effects of factors such as pore size and coating composition on the bioactivity of PEEK-HAp composites, whilst maintaining the balance of mechanical properties.

4.2. 3D Printed Porous Structures

Spece et al. [45] limited pore size to 600 μm, but varied the shape of the pore to examine its effect, with rectangular, gyroid and diamond shapes inspected. A significant increase in alkaline phosphate (ALP) assay cell was seen versus solid PEEK, for all pore shapes, over both 7 and 14 days. With a diamond pore shape showing a non-significant increase over the other shapes. Liu et al. [87] explored a 700 μm pore size, but did not comment on any possible variation. Li et al. [88] determined that 600 μm was the optimal pore size, any larger would decrease the solid area and weaken the porous area on cell growth, and a smaller diameter would have insufficient oxygen and nutrient contents. Feng et al. [44] suggested that a pore size of 300–450 μm enhances cell adhesion and osteogenic differentiation, and that 450–600 μm is preferential for cell proliferation with 450 μm favoured for bone ingrowth and vascular perfusion in-vivo.

Wong et al. [89] explores various porosities 40–60% via FFF with 40% optimizing bone compatibility. Which is similar to Li et al. [88], but lower than results presented by Spece et al. [45]. With lower porosity allowing a shorter mineralisation process [89]. Su et al. [90] explored the possibility of enhancing the 3D printed PEEK structures biological activity via sulfonication, creating microscale pore structures on the scaffold surfaces, with successful results. PEEK scaffolds could also be a promising avenue for alveolar bone augmentation, with similar osteogenic space maintenance versus titanium, but with reduced stiffness that still needs to be improved, Li et al. [91]. Shilov et al. [92] discovered that a higher print resolution (smaller nozzle) increased cell adhesion and Roskies et al. [93] incorporated a trabecular network into PEEK via SLS but care needs to be taken with material shrinkage, reducing the original pore size.

The reviewed papers demonstrate various approaches to create porous PEEK structures, modify the surface bioactivity, and evaluate the mechanical and biological properties of the resulting scaffolds. These modifications have shown potential to improve cell activity, bone ingrowth, and implant-tissue bonding interfaces. However, further studies are needed to determine the optimal pore size, porosity, and geometry for the specific area of bone targeted.

The studies noted here have demonstrated the effectiveness of 3D printed porous PEEK, opening the possibility for the creation of patient-specific implants with tailored porosity. The future work in this area should prioritise exploring the effects of varied pore size and geometries to induce a combination of early-phase cell and strong tissue attachments. The use of both micro and macro pores in combination could potentially lead to more optimal outcomes while maintaining acceptable mechanical properties for the selected region of defected bone.

4.3. Plasma

Plasma treatment can enhance PEEK bioactivity and hydrophilicity without altering its physical properties. Surface oxygen content, chemistry, and charge are altered by the process [15]. Han et al. [15] used Argon or Oxygen (O_2) plasma to increase the level of PEEK bioactivity, both successful but O_2 more so, the authors ascribe this to the ability of O_2 plasma bringing in hydrophilic groups to stimulate adhesion and proliferation of osteoblasts. All whilst maintaining the physical bulk properties of the material due to the non-invasive nature of the treatment. Another plasma technique using plasma ion implantation was

Table 2
An in-vitro and in-vivo AM PAEK biological activity summary.

Study	Material	AM	Bio increase process	Vivo or vitro	Assessment
Composites					
2019 Han [49]	CFR-PEEK	FDM (FFF)	5% CF 80–150 μm Ø7 μm	In-vitro	L929 DMEM -CCK-8
2020 Alam [51]	PEEK-CNT & GNPs	FDM(FFF)	1 wt% CNT 3 wt% GNP	In-vitro	SBF apatite formation
2021 Zheng [55],	PEEK/HAp	FFF	PEEK:HAp 8:2,6:4 – Wt% ratio	In-vitro	MC3T3-E1
2021 Rodzen [56],	PEEK/HAp	FFF	30 wt% HAp	In-vitro	U-2 OS
2020 Sikder [58],	AMP - PEEK FILAMENT	FILAMENT		In-vitro Rats	MC3T3-E1 osseointegration
2021, Oladapo [61]	PEEK/rGO/cHAp	FDM(FFF)	1–5 wt% rGO	In-vitro	L929 DMEM
2022 Manzoor [64],	PEEK Zn-nanoHAp	FDM (FFF)	10–20 wt% ZnHAp	In-vitro	SBF apatite formation
2021 Manzoor [65]	PEEK/HAp	FDM (FFF)	pure nano-HAp (Sr) nano-HAp (Zn)nano-HAp	In-vitro	SBF apatite formation
2020 Oladapo [79],	PEEK - cHAp	FDM – FFF	cHAp powder	In-vitro	MG-63
2022 Hu [80],	AMX-loaded HAp-coated PEEK	3 M V2	Nano-Hap – hydrothermal coating AMX solution	In-vitro	rASCs CCK-8 kit Antibacterial
2019 Zhong [81],	PEEK/HAp	HAp scaffold PEEK Compression moulded PEEK		In-vitro	DOESN'T DEFINE CELL
2022 Zheng [82]	PEEK/HAp	FDM (FFF)	0,20,40 wt% HAp 400–500 μm Pores	In-vitro Rabbits	BMSCs
2018 Feng [83]	PEEK/ β-TCP + PLLA	SLS	20% β-TCP 0–50 wt% PLLA	In-vitro Rabbits	SBF – apatite formation MG-63 osseointegration
2020 Gao [84],	PEK-CN/nHAp	FDM(FFF)	0–5 wt% nHAp	In-vitro	CCK-8 MC3T3-E1 L929
2022 GAO [85]	PAEK-COOH Bio ink	Low temp DM		In-vitro Rabbits	MC3T3-E1
Porous					
2020, Feng [44]	PEEK	FDM (FFF)	300,450,600 μm Pores 60% porosity	In-vitro Rabbits	hBMSCs CCK-8 kit
2020 Spece [45],	PEEK	FFF	Porosity 70–74% 600 μm struts	In-vitro	MC3T3-E1 preosteoblast cells
2022, Liu [87]	PEEK – CSMA/POSS	FFF	700 μm Pores 2% w/v CSMA 0–4% *w/v* POSS	In-vitro RAT	rBMSCs CCK-8 kit
2021 Li [88],	PEEK	FDM 3DP (FFF)	Pore Diameter 0.4–0.6 mm	In-vitro	Osteoblast precursor cells (MC3T3-E1)
2021 Wong [89]	PEEK	FDM (FFF)	Porosity 40–60%	In-vitro and rabbit	MC3T3-E1 Histological osseointegration
2020 Su [90],	PEEK	FFF	Sulfonication 15 – 180s on Lattice structures	In-vitro Rabbit	MC3T3-E1 osseointegration
2022 Li [91]	PEEK	FDM (FFF)	Scaffolds	In-vivo	Beagles
2022 Shilov [92]	PEEK	FFF	Print resolution - via nozzle diameter	In-vitro	Cell viability/bioactivity Rat – Peritoneal & Bone marrow cells
2016 Roskies [93],	PEEK	SLS	Scaffold	In-vitro	ADSCs BMSCs
Plasma					
2022 Han [15]	PEEK	FFF	Plasma – Ar, O2	In-vitro	SAOS-2 Osteoblasts
2020 Kruse [94]	PEEK	AON-M2 (FFF)	Plasma – PIII In N gas	In-vitro	SAOS-2 Osteoblasts
2021 Liu [95]	PEEK	FDM(FFF)	Etched 02 plasma.	In-vitro Rabbits	L929 osseointegration
Sanblasting					
2022 Limaye [16]	PEEK	FDM (FFF)	Sandblast Alumina 50,125 μm	In-vitro	HUVEC and HOBs
2019 Han [17]	PEEK	FFF	Sandblast Alumina 50,120,250 μm	In-vitro	SAOS-2 osteoblasts

(*continued on next page*)

Table 2 (*continued*)

Study	Material	AM	Bio increase process	Vivo or vitro	Assessment
Grafting					
2023 Zhang [96]	PEEK	FFF	Sandpaper Grafting. PAA + EDA	In-vitro	BMSCs MFBs Cytotoxicity + proliferation
Coatings					
2019 Jung [60]	PEEK	FDM (FFF)	Ti Coating -sputtering	In-vitro rabbits	MC3T3-E1 Osseointegration – bone regeneration
2022 CvrČek [75]	PEEK – TiNb coating	SLS	TiNB	In-vitro	Saos-2 Cells

used [94], covalently linking the protein to the PEEK surface, alongside increased hydrophilicity. Plasma treatment increases the hydrophilicity and creates a micro and nano topographical surface that is key to enhancing cell adhesion [15]. This treatment is also beneficial as plasma can vary the morphology of the surface without altering the materials average roughness [95]. It is noted that increases in content of surface oxygen could also be a key factor in creating a hydrophilic surface, alongside the surface chemistry and charge being altered by the process of plasma treatment.

4.4. Sandblasting

Untreated FFF PEEK outperformed sandblasted groups in cell metabolic activity, proliferation, and osteoblast density [17]. The roughness of the untreated material was 22.28 μm, equal to that of the tested cell size. This is contradicted by Limaye et al. [16] showing that the sandblasting with 50 and 125 μm silica particles removed printing defects and created roughened surfaces for increased uniform cell adhesion and distribution. The increase in performance is suggested to be due to the higher surface roughness and optimal printing structures. When the average roughness of the surface is equal to that of the cell size it can lead to increased cell proliferation, allowing the cells to slide and attach into the valleys, from a dense initial cell layer.

The only variance in the printing parameters, is the layer thickness, with 0.2 mm [17] for and 0.1 mm for [16]. As such the latter may have a smoother surface finish. The authors suggest that this contraction could be due to the various roughness values that can be produced by FFF printing depending on the parameters. So, post treatment using sandblasting may move the overall roughness closer to or further away from the optimal value required for enhanced bioactivity. Roughness should be optimised for the outcome required from the sample and tied in with the mechanical properties of the sample.

Super hydrophilic PEEK via surface grafting (PAA and EDA) was assessed [96], and showed that a hydrophilic surface on its own is not enough to promote cellular affinity. It was noted by the authors that wettability affects the initial phase of cell adhesion, and the topography affects long term adhesion and proliferation [97,98].

Finally [60], coated 3D printed PEEK in titanium with superior biological activity versus the untreated printed surface, by increasing the surfaces' wettability [99]. This process does however re-establish the presence of metal in the implant, which contrasts the aims of a polymer device.

4.5. Bioactivity Overview

This section reviews the various approaches to modify the surface characteristics of 3D-printed PEEK implants to improve their biocompatibility, osseointegration, and other desirable properties. It highlights the importance of enhancing the bioactivity of PEEK implants and suggests the addition of HAp to the PEEK matrix to achieve this. The studies presented in this reviewed indicate that the addition of HAp to the PEEK matrix can lead to increased surface apatite formation, improved cell adhesion, and potential for bone tissue repair. The optimal percentage of HAp varies between studies, with some showing improved properties at 10 wt%, while others suggest higher levels such as 15 wt% or 30 wt%. Other additives, such as Zinc, can also be incorporated into the PEEK matrix to enhance its properties. The report also highlights the importance of pore size in enhancing cell growth, with the optimal pore size varying between 150 and 1200 μm. The report suggests that further research is needed to investigate the effects of factors such as pore size and coating composition on the bioactivity of PEEK-HAp composites, whilst maintaining the balance of mechanical properties.

4.6. Suggested Future Work

After presenting the current field of literature, some potential future research directions for increasing the biological activity of 3D printed PEEK include:

Investigating the effects of different surface modification techniques in combination with PEEK-HAp composites on cellular behaviour.

Exploring the use of other bioactive additives, in PEEK composites to enhance bone regeneration and antimicrobial properties.

Optimizing the pore size and shape in 3D printed PEEK scaffolds to ensure both cell adhesion, osteoblast proliferation and vascularisation are promoted. Also, to link this with the wettability and topographical characteristics discussed.

Studying the long-term biocompatibility and osseointegration of 3D printed PEEK implants in-vivo to evaluate their clinical potential and safety. Alongside this, the mechanical and biological properties of PEEK composites under dynamic loading conditions should be further studied to simulate physiological environments and better predict their clinical performance.

5. Conclusion

In conclusion, this comprehensive review highlights the persistent mechanical performance disparity between 3D-printed thermoplastic components, particularly polyetheretherketone (PEEK), and their conventional counterparts, with 3D-printed parts exhibiting lower tensile (approximately 76.5%) and flexural strength and fracture toughness. This disparity is attributed to inherent anisotropy within additive materials, leading to a heightened likelihood of surface defects, thereby increasing the probability of failure. The insufficiency of studies exploring the tribological behaviour of 3D-printed PAEKs in load-bearing orthopaedic applications, the absence of biologically representative lubricants such as FBS, and the predominance of short-term testing underscore the need for more clinically relevant assessments.

The Key findings are summarized as follows:

Surface modification techniques, particularly the incorporation of hydroxyapatite (HAp) into the PEEK matrix, have shown promise in enhancing biocompatibility and cellular adhesion, with optimal HAp percentages varying (e.g., 10 wt%, 15 wt%, 30 wt%). Additionally, pore size in PEEK-HAp composites, ranging from 150 μm to 1200 μm,

significantly influences cell growth.

It has been noted that future research directions encompass investigating various surface modification techniques in combination with PEEK-HAp composites, exploring alternative bioactive additives for enhanced bone regeneration and antimicrobial properties, optimizing scaffold pore size and shape to promote cell adhesion and vascularization, and conducting in-vivo assessments to evaluate long-term biocompatibility and osseointegration while subjecting PEEK composites to dynamic loading conditions for more accurate clinical performance predictions.

Credit authorship contribution statement

Benjamin A. Clegg: Conceptualization, Methodology, Investigation, Writing – original draft, Visualization. **Dilesh Raj Shrestha:** Conceptualization, Methodology, Investigation, Writing – original draft, Visualization. **Nazanin Emami:** Resources, Writing – review & editing, Supervision, Project administration, Funding acquisition.

Declaration of Competing Interest

The authors declare no conflicts of interest.

Data availability

Data will be made available on request.

Acknowledgements

This project has received funding from the European Union's Horizon 2020 Research and innovation programme under grant agreement No. 956004.

Appendix A. 3D Printing of Neat PAEK

References	Material	Method	Printing parameters (optimised)		Properties (optimum)		Comment
			Parameters	Value	Parameters	Value	
[5]	PEEK	FFF	Nozzle temperature Bed temperature Print speed	427 °C 160 °C 20 mm/s	Porosity Young's modulus Stress at break	1.18% 4.8 GPa 66 MPa	Brittle nature of fracture was present in PEEK which might be downside for load bearing application purposes.
[14]	PEEK	FFF	Nozzle temperature, Bed temperature, Ambient temperature	400–430 °C, 130 °C, 80 °C	Compressive yield strength (0% porosity), Compressive yield strength (38% porosity) Flexural modulus Flexural strength	102.38 MPa 29.34 MPa 2.43 GPa 132.37 MPa	Due to the air gap/porosity, the 3D printed possesses reduction in properties compared to Injection moulded.
[16]	PEEK	FFF	Nozzle temperature Print speed Bed temperature	485 °C 33.3 mm/s 130 °C	Tensile strength Flexural strength Vickers hardness	53.91 MPa 182.79 MPa 29.3 HV	Post treatment like sandblasting can improve mechanical as well as biocompatibility of 3D printed PEEK
[24]	PEEK	FFF	Print speed Layer thickness Printing temperature Filling rate	60 mm/s 0.25 mm 370 °C 60 %	Tensile strength Elongation Bending strength Impact strength	40 MPa 14.3% 68.2 MPa 101.2 KJ/m [2]	For compressive analysis, the optimum parameters were different.
[25]	PEEK	FFF	Nozzle temperature Print speed Layer thickness Nozzle Ø	440 °C 20 mm/s 0.1 mm 0.4 mm	Tensile strength Density	76 MPa 92%	Increasing nozzle temperature and decreasing the print speed and layer height will yield high performing material
[27]	PEEK	FFF	Nozzle temperature Bed temperature Print speed Layer thickness	415 °C 160 °C 50 mm/s 0.2 mm	Max Tensile strength (Taguchi)	48.9 MPa	Taguchi approach was used along with the experiment approach which were in good agreement with each other.
[28]	PEKK	FFF	Build orientation. Infill pattern Raster angle Counters	Flat Lines ±45° 2	Young's modulus UTS Elongation at break	1782 MPa 79.8 7.87%	Porosity was higher with the sample printed on edge orientation than the flat.
[29]	PEEK	High temp. LS	Build orientation	Horizontal Inverted-horizontal	Uniaxial static compression mode (Highest) Density (Highest) Dimensional accuracy (Highest)	Inverted-horizontal. Horizontal Horizontal	Inverted-Horizontal and Horizontal build direction showed better accuracy and mechanical performance.
[30]	PEEK	FFF	Build orientation (H, V) Raster angle (0°, 90°)	Horizontal 0°	Tensile strength Flexural strength Fracture toughness	82.58 MPa 142 MPa 5.32 MPa.$m^{1/2}$	Represents different thermal gradient between beads printing with different configurations
[31]	PEEK	FFF	Nozzle temperature Print speed (mm/min)	435 °C 2100 145 °C	**With nozzle 0.4 mm and infill angle 180° and with heat treatment** Elastic modulus Tensile strength	8.06 GPa 128.15 MPa	Infill angle of 180° showed the highest levels of tensile strength and modulus of elasticity.

(*continued on next page*)

(*continued*)

References	Material	Method	Printing parameters (optimised)		Properties (optimum)		Comment
			Parameters	Value	Parameters	Value	
			Bed temperature Chamber temperature Layer height	75 °C 0.1 mm			
[32]	PEEK	FFF	Nozzle temperature Print speed Bed temperature Layer thickness	485 °C 30 mm/s 100 °C 0.1 mm	Tensile strength Flexural strength Shear strengths	76.5 MPa 149.7 MPa 55.5 MPa	Effect of raster angle was investigated as it is one of the main parameters for determining mechanical strength.
[33]	PEEK	FFF	Nozzle temperature Print speed Layer thickness Extrusion width	395 °C 5 mm/s 0.1 mm 0.44 mm	Tensile strength Porosity (before and after annealing)	91.48 MPa 0.3 to 3.9%	No effect on crystallinity with all the printing parameters
[34]	PEEK	FFF	Nozzle temperature Bed temperature Chamber temperature Print speed	380 °C 130 °C 65 °C 15 mm/s	Defect volume ratio for design with Wall line count: 1 Infill density: 100% Raster angle: ±45°	0.06%	Printed with layer height 0.2 mm varying the wall line count, infill density and raster angle.
[35]	PEEK	FFF	Ambient temperature Substrate temperature	90 °C 160 °C	Interlayer bonding force Tensile strength Bending strength	989.91 N 86.62 MPa 113.21 MPa	The influence of substrate temperature was greater than ambient temperature.
[37]	PEEK	FFF	Nozzle temperature Chamber temperature With heat collector	400 °C 135 °C	Tensile strength Elastic modulus Bending strength	74.7 MPa 1150 MPa 120.2 MPa	High temperature chamber, nozzle with a heat collector module and platform ensures the reliable manufacturing process.
[38]	PEEK	Screw extrusion	Nozzle temperatures Heated plate Extrusion rate	370–390 °C 280 °C 1.5 g/min	Tensile strength (Nozzle 390 °C) Compressive strength (Nozzle 390 °C)	94 MPa 140 MPa	New additive manufacturing system 96% of bulk strength achieved
[39]	PEEK	FFF	Layer height Nozzle temperature Bed temperature	0.1 mm 390–410 °C 100 °C	Lower print speed and annealing Higher print speed and annealing	Increased properties No significant effect	Higher print speed (2000 mm/min) might result to better interlayer adhesion showing no effect of annealing
[40]	PEEK	FFF	Nozzle temperature Print speed Bed temperature	420 °C 20 mm/s 0.2 100 °C/ 140 °C	Tensile strength Flexural strength	82 MPa 141 MPa	With annealing crystallinity is improved increasing the tensile strength of the material.
[41]	PEEK	FFF	Nozzle temperature Print speed Layer height Wait time	410 °C 20 mm/s 0.1 mm 11 s	Flexural stress at break and strain at break Flexural stress/strain at break	Strong correlation No significant correlation	Flexural stress/strain can indicate materials interlayer bonding strength
[42]	PEEK	FFF	Nozzle Ø Nozzle temperature Print speed	0.2–0.6 mm 420–440 °C 5–15 mm/s	Bending strength Compression strength Elastic modulus	193.33 MPa 87 MPa 2.193 GPa	Different parameter combinations are found to obtain optimal mechanical properties.
[43]	PEEK	FFF	Nozzle Ø Printing temperature Print speed Layer thickness	0.3 mm 420 °C 18 mm/s 0.25 mm	Density, tensile strength, and surface improved with increasing nozzle temperature, decreasing print speed and reduced layer thickness.		Preliminary values from FEA, Nozzle temperature: 360–420 °C Print speed: 16 to 22 mm/s Layer thickness: 0.1 to 0.35 mm
[44]	PEEK	FFF	Nozzle temperature Layer thickness Average pore sizes	480 °C 0.1 mm 300 -600 μm	Compressive strength for 300 μm pore sizes Compressive strength for 600 μm pore sizes Wettability	59.9 MPa 31.2 MPa Increases with pore sizes	Mechanical properties of porous PEEK closely matched with human trabecular bone
[45]	PEEK	FFF	Nozzle temperature Layer height Print speed Nozzle size	420–450 °C 0.1 mm 2200 mm/min 0.2 mm	Yield strength (Rectilinear) Yield strength (Gyroid) Yield strength (Diamond)	6.6 MPa 14.8 MPa 17.1 MPa	Smaller pore size was with the rectilinear design and lower rougher surface was with the gyroid printed specimen.
[46]	PEEK	PBF	Laser power Laser scan speed Layer thickness	25 W 2000 mm/s 0.1 mm	Elastic modulus (MPa) Yield strength	42.17 -512.12 1.9 -22.42 MPa	Gyroid, diamond and I-WP pore structure were evaluated.

Appendix B. PAEK 3D Printed Composites

References	Material	Method	Printing parameters (optimised)		Properties (optimum)		Comments
			Parameters	Value	Parameters	Value	
[55]	PEEK/HA	FFF	Nozzle temperature: Layer thickness Print speed	420 °C 0.1 mm 30 mm/s	Young's modulus Strength *By increasing the pore size from 0.2 to 2.0 mm*	624.7-50.6 MPa 35.2 -2.2 MPa	Crystallinity increases with increase of HAp content
[48]	PEEK/HAp	FFF	Nozzle temperature Print speed Nozzle dia Layer height Bed/chamber temp Raster angle	400 °C 40 mm/s 1 mm 0.1 mm 280/230 °C ±45° XY	**PEEK** Tensile modulus Flexural modulus **PEEK 30 wt%** Tensile modulus Flexural modulus	4241 MPa 4274 MPa 6110 MPa 5686 MPa	Up to 30 wt% PEEK/HAp composite can be printed.
[49]	PEEK/CF	FFF	Nozzle temperature Print speed Layer thickness Ambient temperature	420 °C 40 m/s 0.2 mm 20 °C	**Tensile modulus:** PEEK CFR PEEK	3.79 GPa 7.37 GPa	Surface modification (polishing and sandblasting) improved the hydrophilic behaviour.
[50]	PEEK/CNT PEEK/GNP	FFF	Nozzle temperature Print speed Layer thickness Extrusion width Bed temperature	390 °C 1000 mm/min 0.1 mm 0.48 mm 100 °C	**For GNP 3 wt%** Young's modulus CoF **For CNT 1 wt%** Young's modulus CoF	3.68 GPa 0.1 3.37 GPa 0.08	CNT/GNP reinforced PEEK composites exhibit higher wear rate compared to neat PEEK.
[51]	PEEK/ CNT/GNP	FFF	Nozzle temperature Print speed Extrusion width Layer height Bed temperature	410 °C 1000 mm/min 0.48 mm 0.1 mm 100 °C	**For GNP 3 wt% non-sulphonated** Young's modulus **For CNT 1 wt% non-sulphonated** Young's modulus	3.96 GPa 3.85 GPa	Sulfonation no significant effect on crystallinity while reinforcement increased the crystallinity.
[52]	PEEK/GnP	FFF	PEEK filaments Extrusion temperature	380–400 °C	**PEEK/GnP 1 wt%** UTS Young's modulus Storage modulus	139 MPa 2525 MPa 3958 MPa	Addition of GnP enhanced the thermal stability
[54]	PEEK/CF	FFF	Nozzle temperature Print speed Layer thickness Ambient temperature Bed temperature	400 °C 15 mm/s 0.1 mm 90 °C 160 °C	Bending strength (Vertically printed) CF/PEEK	146 MPa	Vertically printed PEEK and its CF reinforced composites show strengths as high as moulded composites.
[59]	PEEK/ HAp/GO	FFF	Nozzle temperature Print speed Extrusion width Chamber temperature Bed temperature	390 °C 3000 mm/min 0.48 mm 90 °C 160 °C	Porosity Tensile strength	1.2% 67 MPa	The strength between the fibre and the matrix is relatively low.
[60]	PEEK/Ti coated	FFF	Nozzle temperature Print speed Layer thickness Ambient temperature	400 °C 20 mm/s 0.2 mm 160 °C	Tensile strength Young's modulus	84.1 MPa 2.42 GPa	Ti-modified surfaces enhance the interfacial biocompatibility

References

[1] S.M. Kurtz (Ed.), PEEK Biomaterials Handbook, Second, William Andrew, 2019.

[2] S. Singh, C. Prakash, S. Ramakrishna, 3D printing of polyether-ether-ketone for biomedical applications, Eur. Polym. J. 114 (2019) 234–248, https://doi.org/10.1016/J.EURPOLYMJ.2019.02.035.

[3] J. Kang, J. Zhang, J. Zheng, L. Wang, D. Li, S. Liu, 3D-printed PEEK implant for mandibular defects repair - a new method, J. Mech. Behav. Biomed. Mater. (2021) 116, https://doi.org/10.1016/j.jmbbm.2021.104335.

[4] D. Liu, J. Fu, H. Fan, et al., Application of 3D-printed PEEK scapula prosthesis in the treatment of scapular benign fibrous histiocytoma: a case report, J. Bone Oncol. 12 (2018) 78–82, https://doi.org/10.1016/J.JBO.2018.07.012.

[5] S. Petersmann, M. Spoerk, W. Van De Steene, et al., Mechanical properties of polymeric implant materials produced by extrusion-based additive manufacturing, J. Mech. Behav. Biomed. Mater. (2020) 104, https://doi.org/10.1016/j.jmbbm.2019.103611.

[6] B.I. Oladapo, S.A. Zahedi, S.O. Ismail, F.T. Omigbodun, 3D printing of PEEK and its composite to increase biointerfaces as a biomedical material- a review, Colloids Surf. B: Biointerfaces 203 (2021), 111726, https://doi.org/10.1016/J.COLSURFB.2021.111726.

[7] C. Basgul, T. Yu, D.W. Macdonald, R. Siskey, M. Marcolongo, S.M. Kurtz, Structure–property relationships for 3D-printed PEEK intervertebral lumbar cages produced using fused filament fabrication, J. Mater. Res. 33 (14) (2018) 2040–2051, https://doi.org/10.1557/JMR.2018.178.

[8] M. Mbogori, A. Vaish, R. Vaishya, A. Haleem, M. Javaid, Poly-ether-ether-ketone (PEEK) in orthopaedic practice- a current concept review, J. Orthop. Rep. 1 (1) (2022) 3–7, https://doi.org/10.1016/J.JOREP.2022.03.013.

[9] A. Haleem, M. Javaid, Polyether ether ketone (PEEK) and its manufacturing of customised 3D printed dentistry parts using additive manufacturing, Clin.

Epidemiol. Glob. Health 7 (4) (2019) 654–660, https://doi.org/10.1016/J.CEGH.2019.03.001.
[10] R. Harting, M. Barth, T. Bührke, R.S. Pfefferle, S. Petersen, Functionalization of polyetheretherketone for application in dentistry and orthopedics, BioNanoMaterials 18 (1–2) (2017), https://doi.org/10.1515/BNM-2017-0003/ASSET/GRAPHIC/J_BNM-2017-0003_FIG_004.JPG.
[11] S. Bose, S. Vahabzadeh, A. Bandyopadhyay, Bone tissue engineering using 3D printing, Mater. Today 16 (12) (2013) 496–504, https://doi.org/10.1016/J.MATTOD.2013.11.017.
[12] N. Sharma, S. Aghlmandi, S. Cao, C. Kunz, P. Honigmann, F.M. Thieringer, Quality characteristics and clinical relevance of in-house 3D-printed customized polyetheretherketone (PEEK) implants for craniofacial reconstruction, J. Clin. Med. 9 (9) (2020) 1–17, https://doi.org/10.3390/jcm9092818.
[13] M. Vaezi, S. Yang, A novel bioactive PEEK/HA composite with controlled 3D interconnected HA network, Int. J. Bioprinting 1 (1) (2015) 66–76, https://doi.org/10.18063/IJB.2015.01.004.
[14] M. Vaezi, S. Yang, Extrusion-based additive manufacturing of PEEK for biomedical applications, Virtual Phys. Prototyp. 10 (3) (2015) 123–135, https://doi.org/10.1080/17452759.2015.1097053.
[15] X. Han, N. Sharma, S. Spintzyk, et al., Tailoring the biologic responses of 3D printed PEEK medical implants by plasma functionalization, Dent. Mater. 38 (7) (2022) 1083–1098, https://doi.org/10.1016/j.dental.2022.04.026.
[16] N. Limaye, L. Veschini, T. Coward, Assessing biocompatibility & mechanical testing of 3D-printed PEEK versus milled PEEK, Heliyon 8 (12) (2022), https://doi.org/10.1016/j.heliyon.2022.e12314.
[17] X. Han, N. Sharma, Z. Xu, et al., An in vitro study of osteoblast response on fused-filament fabrication 3D printed PEEK for dental and Cranio-maxillofacial implants, J. Clin. Med. 8 (6) (2019), https://doi.org/10.3390/jcm8060771.
[18] ISO/ASTM 52900:2021(en), Additive Manufacturing — General Principles — Fundamentals and Vocabulary, Accessed June 7, 2023, https://www.iso.org/obp/ui/#iso:std:iso-astm:52900:ed-2:v1:en, 2021.
[19] P. Parandoush, D. Lin, A review on additive manufacturing of polymer-fiber composites, Compos. Struct. 182 (2017) 36–53, https://doi.org/10.1016/J.COMPSTRUCT.2017.08.088.
[20] A. Chadha, M.I. Ul Haq, A. Raina, R.R. Singh, N.B. Penumarti, M.S. Bishnoi, Effect of fused deposition modelling process parameters on mechanical properties of 3D printed parts, World J. Eng. 16 (4) (2019) 550–559, https://doi.org/10.1108/WJE-09-2018-0329/FULL/PDF.
[21] J.W. Stansbury, M.J. Idacavage, 3D printing with polymers: challenges among expanding options and opportunities, Dent. Mater. 32 (1) (2016) 54–64, https://doi.org/10.1016/J.DENTAL.2015.09.018.
[22] F. Zhao, D. Li, Z. Jin, Preliminary Investigation of Poly-Ether-Ether-Ketone Based on Fused Deposition Modeling for Medical Applications, Materials 11 (2) (2018) 288, https://doi.org/10.3390/MA11020288, 2018, Vol 11, Page 288.
[23] C. Basgul, H. Spece, N. Sharma, F.M. Thieringer, S.M. Kurtz, Structure, properties, and bioactivity of 3D printed PAEKs for implant applications: a systematic review, J Biomed Mater Res B Appl Biomater 109 (11) (2021) 1924–1941, https://doi.org/10.1002/jbm.b.34845.
[24] X. Deng, Z. Zeng, B. Peng, S. Yan, W. Ke, Mechanical properties optimization of poly-ether-ether-ketone via fused deposition modeling, Materials 11 (2) (2018), https://doi.org/10.3390/MA11020216.
[25] P. Wang, B. Zou, H. Xiao, S. Ding, C. Huang, Effects of printing parameters of fused deposition modeling on mechanical properties, surface quality, and microstructure of PEEK, J. Mater. Process. Technol. 271 (2019) 62–74, https://doi.org/10.1016/J.JMATPROTEC.2019.03.016.
[26] R. Kumar, G. Singh, A. Chinappan, et al., On mechanical, physical, and bioactivity characteristics of material extrusion printed polyether ether ketone, J. Mater. Eng. Perform. (2022), https://doi.org/10.1007/s11665-022-07519-4. Published online.
[27] M. Tafaoli-Masoule, M. Shakeri, S.A. Zahedi, M. Vaezi, Experimental investigation of process parameters in polyether ether ketone 3D printing, Proc. Inst. Mech. Eng. E: J. Process Mech. Eng. (2022), https://doi.org/10.1177/09544089221141554. Published online.
[28] K. Rashed, A. Kafi, R. Simons, S. Bateman, Effects of fused filament fabrication process parameters on tensile properties of polyether ketone ketone (PEKK), Int. J. Adv. Manuf. Technol. 122 (9–10) (2022) 3607–3621, https://doi.org/10.1007/S00170-022-10134-1/TABLES/11.
[29] S. Berretta, K. Evans, O. Ghita, Additive manufacture of PEEK cranial implants: manufacturing considerations versus accuracy and mechanical performance, Mater. Des. 139 (2018) 141–152, https://doi.org/10.1016/J.MATDES.2017.10.078.
[30] M.F. Arif, S. Kumar, K.M. Varadarajan, W.J. Cantwell, Performance of biocompatible PEEK processed by fused deposition additive manufacturing, Mater. Des. 146 (2018) 249–259, https://doi.org/10.1016/J.MATDES.2018.03.015.
[31] I. Vindokurov, Y. Pirogova, M. Tashkinov, V.V. Silberschmidt, Effect of heat treatment on elastic properties and fracture toughness of fused filament fabricated PEEK for biomedical applications, Polymers (Basel) 14 (24) (2022), https://doi.org/10.3390/polym14245521.
[32] S. Gao, R. Liu, H. Xin, H. Liang, Y. Wang, J. Jia, The surface characteristics, microstructure and mechanical properties of peek printed by fused deposition modeling with different raster angles, Polymers (Basel) 14 (1) (2022), https://doi.org/10.3390/polym14010077.
[33] C.P. Jiang, Y.C. Cheng, H.W. Lin, Y.L. Chang, T. Pasang, S.Y. Lee, Optimization of FDM 3D printing parameters for high strength PEEK using the Taguchi method and experimental validation, Rapid Prototyp. J. 28 (7) (2022) 1260–1271, https://doi.org/10.1108/RPJ-07-2021-0166.
[34] C.S. Emolaga, S.A.C. Arañez, P.A.N. de Yro, et al., Surface design of 3D-printed PEEK by controlling slicing parameters, Int. J. Mech. Eng. Robot. Res. (2022) 181–186, https://doi.org/10.18178/ijmerr.11.3.181-186. Published online.
[35] H. Qu, W. Zhang, Z. Li, et al., Influence of thermal processing conditions on mechanical and material properties of 3D printed thin-structures using PEEK material, Int. J. Precis. Eng. Manuf. 23 (6) (2022) 689–699, https://doi.org/10.1007/s12541-022-00650-1.
[36] A. Saini, K. Elhattab, S.K. Gummadi, G.R. Nadkarni, P. Sikder, Fused filament fabrication-3D printing of poly-ether-ether-ketone (PEEK) spinal fusion cages, Mater. Lett. (2022) 328, https://doi.org/10.1016/j.matlet.2022.133206.
[37] B. Hu, X. Duan, Z. Xing, et al., Improved design of fused deposition modeling equipment for 3D printing of high-performance PEEK parts, Mech. Mater. (2019) 137, https://doi.org/10.1016/J.MECHMAT.2019.103139.
[38] J.W. Tseng, C.Y. Liu, Y.K. Yen, et al., Screw extrusion-based additive manufacturing of PEEK, Mater. Des. 140 (2018) 209–221, https://doi.org/10.1016/J.MATDES.2017.11.032.
[39] C. Basgul, T. Yu, D.W. MacDonald, R. Siskey, M. Marcolongo, S.M. Kurtz, Does annealing improve the interlayer adhesion and structural integrity of FFF 3D printed PEEK lumbar spinal cages? J. Mech. Behav. Biomed. Mater. (2020) 102, https://doi.org/10.1016/J.JMBBM.2019.103455.
[40] D. Zhao, T. Li, H. Zhang, W. Liu, G. Yue, L. Pan, Effects of processing parameters and annealing on the mechanical properties of polyether ether ketone(PEEK) via fused deposition modeling(FDM), in: 2021 3rd International Academic Exchange Conference on Science and Technology Innovation, IAECST 2021, Institute of Electrical and Electronics Engineers Inc., 2021, pp. 1020–1026, https://doi.org/10.1109/IAECST54258.2021.9695585.
[41] C.Y. Liaw, J.W. Tolbert, L.W. Chow, M. Guvendiren, Interlayer bonding strength of 3D printed PEEK specimens, Soft Matter 17 (18) (2021) 4775–4789, https://doi.org/10.1039/d1sm00417d.
[42] Y. Wang, W.D. Müller, A. Rumjahn, F. Schmidt, A.D. Schwitalla, Mechanical properties of fused filament fabricated PEEK for biomedical applications depending on additive manufacturing parameters, J. Mech. Behav. Biomed. Mater. (2021) 115, https://doi.org/10.1016/j.jmbbm.2020.104250.
[43] C.P. Khunt, M.A. Makhesana, B.K. Mawandiya, K.M. Patel, Investigations on the influence of printing parameters during processing of biocompatible polymer in fused deposition modelling (FDM), Adv. Mater. Process. Technol. 8 (sup2) (2022) 320–336, https://doi.org/10.1080/2374068X.2021.1927651.
[44] X. Feng, L. Ma, H. Liang, et al., Osteointegration of 3D-printed fully porous polyetheretherketone scaffolds with different pore sizes, ACS Omega 5 (41) (2020) 26655–26666, https://doi.org/10.1021/acsomega.0c03489.
[45] H. Spece, T. Yu, A.W. Law, M. Marcolongo, S.M. Kurtz, 3D printed porous PEEK created via fused filament fabrication for osteoconductive orthopaedic surfaces, J. Mech. Behav. Biomed. Mater. (2020) 109, https://doi.org/10.1016/j.jmbbm.2020.103850.
[46] H. Wang, P. Chen, H. Wu, et al., Comparative evaluation of printability and compression properties of poly-ether-ether-ketone triply periodic minimal surface scaffolds fabricated by laser powder bed fusion, Addit. Manuf. (2022) 57, https://doi.org/10.1016/j.addma.2022.102961.
[47] W. Wojnarowska, S. Miechowicz, T. Kudasik, Effect of manufacturing technique on material homogeneity of an implant made of polyetheretherketone, Polimery/Polymers 65 (11−12) (2020) 771–775, https://doi.org/10.14314/POLIMERY.2020.11.3.
[48] K. Rodzeń, P.K. Sharma, A. McIlhagger, et al., The direct 3D printing of functional PEEK/hydroxyapatite composites via a fused filament fabrication approach, Polymers (Basel) 13 (4) (2021) 1–18, https://doi.org/10.3390/polym13040545.
[49] X. Han, D. Yang, C. Yang, et al., Carbon fiber reinforced PEEK composites based on 3D-printing technology for orthopedic and dental applications, J. Clin. Med. 8 (2) (2019), https://doi.org/10.3390/jcm8020240.
[50] M.F. Arif, H. Alhashmi, K.M. Varadarajan, J.H. Koo, A.J. Hart, S. Kumar, Multifunctional performance of carbon nanotubes and graphene nanoplatelets reinforced PEEK composites enabled via FFF additive manufacturing, Compos. B Eng. (2020) 184, https://doi.org/10.1016/J.COMPOSITESB.2019.107625.
[51] F. Alam, K.M. Varadarajan, J.H. Koo, B.L. Wardle, S. Kumar, Additively manufactured polyetheretherketone (PEEK) with carbon nanostructure reinforcement for biomedical structural applications, Adv. Eng. Mater. 22 (10) (2020), https://doi.org/10.1002/adem.202000483.
[52] S. Yaragalla, M. Zahid, J.K. Panda, N. Tsagarakis, R. Cingolani, A. Athanassiou, Comprehensive enhancement in thermomechanical performance of melt-extruded peek filaments by graphene incorporation, Polymers (Basel) 13 (9) (2021), https://doi.org/10.3390/polym13091425.
[53] C. Guo, X. Liu, G. Liu, Surface finishing of fdm-fabricated amorphous polyetheretherketone and its carbon-fiber-reinforced composite by dry milling, Polymers (Basel) 13 (13) (2021), https://doi.org/10.3390/polym13132175.
[54] Q. Li, W. Zhao, Y. Li, W. Yang, G. Wang, Flexural properties and fracture behavior of CF/PEEK in orthogonal building orientation by FDM: microstructure and mechanism, Polymers (Basel) 11 (4) (2019), https://doi.org/10.3390/POLYM11040656.
[55] J. Zheng, H. Zhao, E. Dong, et al., Additively-manufactured PEEK/HA porous scaffolds with highly-controllable mechanical properties and excellent biocompatibility, Mater. Sci. Eng. C (2021) 128, https://doi.org/10.1016/j.msec.2021.112333.
[56] K. Rodzeń, M.J. McIvor, P.K. Sharma, et al., The surface characterisation of fused filament fabricated (Fff) 3d printed peek/hydroxyapatite composites, Polymers (Basel) 13 (18) (2021), https://doi.org/10.3390/polym13183117.

[57] B.I. Oladapo, S.A. Zahedi, S.O. Ismail, Mechanical performances of hip implant design and fabrication with PEEK composite, Polymer (Guildf) (2021) 227, https://doi.org/10.1016/j.polymer.2021.123865.

[58] P. Sikder, J.A. Ferreira, E.A. Fakhrabadi, et al., Bioactive amorphous magnesium phosphate-polyetheretherketone composite filaments for 3D printing, Dent. Mater. 36 (7) (2020) 865–883, https://doi.org/10.1016/j.dental.2020.04.008.

[59] B.I. Oladapo, O.B. Obisesan, B. Oluwole, V.A. Adebiyi, H. Usman, A. Khan, Mechanical characterization of a polymeric scaffold for bone implant, J. Mater. Sci. 55 (21) (2020) 9057–9069, https://doi.org/10.1007/s10853-020-04638-y.

[60] Jung H. Do, T.S. Jang, J.E. Lee, S.J. Park, Y. Son, S.H. Park, Enhanced bioactivity of titanium-coated polyetheretherketone implants created by a high-temperature 3D printing process, Biofabrication 11 (4) (2019), https://doi.org/10.1088/1758-5090/AB376B.

[61] B.I. Oladapo, S.A. Zahedi, Improving bioactivity and strength of PEEK composite polymer for bone application, Mater. Chem. Phys. (2021) 266, https://doi.org/10.1016/j.matchemphys.2021.124485.

[62] B.I. Oladapo, S.O. Ismail, O.K. Bowoto, F.T. Omigbodun, M.A. Olawumi, M. A. Muhammad, Lattice design and 3D-printing of PEEK with Ca10(OH)(PO4)3 and in-vitro bio-composite for bone implant, Int. J. Biol. Macromol. 165 (2020) 50–62, https://doi.org/10.1016/j.ijbiomac.2020.09.175.

[63] C.C. Santiago, B. Yelamanchi, J.A. Diosdado De la Peña, et al., Thermoplastic extrusion additive manufacturing of high-performance carbon fiber peek lattices, Crystals (Basel) 11 (12) (2021), https://doi.org/10.3390/cryst11121453.

[64] F. Manzoor, A. Golbang, A. McIlhagger, E. Harkin-Jones, D. Crawford, E. Mancuso, Effect of Zn-nanoHA concentration on the mechanical performance and bioactivity of 3D printed PEEK composites for craniofacial implants, Plast. Rubber Compos. (2022), https://doi.org/10.1080/14658011.2022.2108986. Published online.

[65] F. Manzoor, A. Golbang, S. Jindal, et al., 3D printed PEEK/HA composites for bone tissue engineering applications: effect of material formulation on mechanical performance and bioactive potential, J. Mech. Behav. Biomed. Mater. (2021) 121, https://doi.org/10.1016/j.jmbbm.2021.104601.

[66] F. Manzoor, A. Golbang, D. Dixon, et al., 3D printed strontium and zinc doped hydroxyapatite loaded PEEK for craniomaxillofacial implants, Polymers (Basel) 14 (7) (2022), https://doi.org/10.3390/polym14071376.

[67] H. Jiang, P. Aihemaiti, W. Aiyiti, A. Kasimu, Study of the compression behaviours of 3D-printed PEEK/CFR-PEEK sandwich composite structures, Virtual Phys. Prototyp. 17 (2) (2022) 138–155, https://doi.org/10.1080/17452759.2021.2014636.

[68] A. Matschinski, P. Ziegler, T. Abstreiter, T. Wolf, K. Drechsler, Fiber formation of printed carbon fiber/poly (ether ether ketone) with different nozzle shapes, Polym. Int. 70 (8) (2021) 1109–1117, https://doi.org/10.1002/PI.6196.

[69] Z. Chen, H. Wang, J. Su, et al., Evaluation of mechanical and biological properties of akermanite/poly-ether-etherketone composite fabricated by hightemperature laser powder bed fusion, Int. J. Bioprinting 9 (3) (2023), https://doi.org/10.18063/ijb.699.

[70] H. Wang, P. Chen, Z. Shu, et al., Laser powder bed fusion of poly-ether-ether-ketone/bioactive glass composites: processability, mechanical properties, and bioactivity, Compos. Sci. Technol. (2023) 231, https://doi.org/10.1016/j.compscitech.2022.109805.

[71] Q. Xu, W. Xu, Y. Yang, et al., Enhanced interlayer strength in 3D printed poly (ether ether ketone) parts, Addit. Manuf. (2022) 55, https://doi.org/10.1016/j.addma.2022.102852.

[72] J. Gonçalves, P. Lima, B. Krause, et al., Electrically Conductive Polyetheretherketone Nanocomposite Filaments: From Production to Fused Deposition Modeling, Polymers 10 (8) (2018) 925, https://doi.org/10.3390/POLYM10080925, 2018, Vol 10, Page 925.

[73] A. Golbang, E. Harkin-Jones, M. Wegrzyn, G. Campbell, E. Archer, A. Mcilhagger, Production and Characterization of PEEK/IF-WS 2 Nanocomposites for Additive Manufacturing: Simultaneous Improvement in Processing Characteristics and Material Properties, Published online, 2019, https://doi.org/10.1016/j.addma.2019.100920.

[74] C. Yang, J. Xu, Y. Xing, S. Hao, Z. Ren, Covalent Polymer Functionalized Graphene Oxide/ Poly(Ether Ether Ketone) Composites for Fused Deposition Modeling: Improved Mechanical and Tribological Performance, Published online, 2020, https://doi.org/10.1039/d0ra04418k.

[75] L. Cvrček, J. Krčil, J. Musílková, et al., Nanostructured TiNb coating improves the bioactivity of 3D printed PEEK, Mater. Des. (2022) 224, https://doi.org/10.1016/j.matdes.2022.111312.

[76] K.A. Laux, Adhesive Wear Phenomena in High Performance Polyaryletherketones (PAEK) Polymers (Doctoral Dissertation), 2016.

[77] A.A. Stratton-Powell, K.M. Pasko, C.L. Brockett, J.L. Tipper, The biologic response to polyetheretherketone (PEEK) wear particles in total joint replacement: a systematic review, Clin. Orthop. Relat. Res. 474 (11) (2016) 2394–2404, https://doi.org/10.1007/s11999-016-4976-z.

[78] D. Bitar, J. Parvizi, Biological response to prosthetic debris, World J. Orthop. 6 (2) (2015) 172, https://doi.org/10.5312/WJO.V6.I2.172.

[79] B.I. Oladapo, S.A. Zahedi, S.O. Ismail, et al., 3D printing of PEEK–cHAp scaffold for medical bone implant, Biodes. Manuf. 4 (1) (2021) 44–59, https://doi.org/10.1007/s42242-020-00098-0.

[80] Q. Hu, Y. Wang, S. Liu, Q. Liu, H. Zhang, 3D printed polyetheretherketone bone tissue substitute modified via amoxicillin-laden hydroxyapatite nanocoating, J. Mater. Sci. 57 (39) (2022) 18601–18614, https://doi.org/10.1007/s10853-022-07782-9.

[81] G. Zhong, M. Vaezi, X. Mei, P. Liu, S. Yang, Strategy for controlling the properties of bioactive poly-ether-ether-ketone/hydroxyapatite composites for bone tissue engineering scaffolds, ACS Omega (2019), https://doi.org/10.1021/acsomega.9b02572. Published online.

[82] J. Zheng, H. Zhao, Z. Ouyang, et al., Additively-manufactured PEEK/HA porous scaffolds with excellent osteogenesis for bone tissue repairing, Compos. B Eng. (2022) 232, https://doi.org/10.1016/j.compositesb.2021.109508.

[83] P. Feng, P. Wu, C. Gao, et al., A multimaterial scaffold with tunable properties: toward bone tissue repair, Adv. Sci. 5 (6) (2018), https://doi.org/10.1002/advs.201700817.

[84] X. Gao, H. Wang, X. Zhang, et al., Preparation of amorphous poly(aryl ether nitrile ketone) and its composites with nano hydroxyapatite for 3D artificial bone printing, ACS Appl. Bio Mater. 3 (11) (2020) 7930–7940, https://doi.org/10.1021/acsabm.0c01044.

[85] X. Gao, H. Wang, S. Luan, G. Zhou, Low-temperature printed hierarchically porous induced-biomineralization polyaryletherketone scaffold for bone tissue engineering, Adv. Healthc. Mater. 11 (18) (2022), https://doi.org/10.1002/adhm.202200977.

[86] X. Gao, H. Wang, S. Luan, G. Zhou, Biofabrication of poly(aryletherketone)-hydroxyapatite composite Scaffolds via low-temperature printing, Adv. Mater. Technol. (2023) 2201676, https://doi.org/10.1002/admt.202201676. Published online April 29.

[87] Z. Liu, M. Zhang, Z. Wang, et al., 3D-printed porous PEEK scaffold combined with CSMA/POSS bioactive surface: a strategy for enhancing osseointegration of PEEK implants, Compos. B Eng. (2022) 230, https://doi.org/10.1016/j.compositesb.2021.109512.

[88] S. Li, T. Wang, J. Hu, et al., Surface porous poly-ether-ether-ketone based on three-dimensional printing for load-bearing orthopedic implant, J. Mech. Behav. Biomed. Mater. (2021) 120, https://doi.org/10.1016/j.jmbbm.2021.104561.

[89] K.I. Wong, Y. Zhong, D. Li, Z. Cheng, Z. Yu, M. Wei, Modified porous microstructure for improving bone compatibility of poly-ether-ether-ketone, J. Mech. Behav. Biomed. Mater. (2021) 120, https://doi.org/10.1016/j.jmbbm.2021.104541.

[90] Y. Su, J. He, N. Jiang, et al., Additively-manufactured poly-ether-ether-ketone (PEEK) lattice scaffolds with uniform microporous architectures for enhanced cellular response and soft tissue adhesion, Mater. Des. (2020) 191, https://doi.org/10.1016/j.matdes.2020.108671.

[91] L. Li, H. Gao, C. Wang, P. Ji, Y. Huang, C. Wang, Assessment of customized alveolar bone augmentation using titanium scaffolds vs polyetheretherketone (PEEK) scaffolds: a comparative study based on 3D printing technology, ACS Biomater. Sci. Eng. (2022), https://doi.org/10.1021/acsbiomaterials.2c00060. Published online.

[92] S.Y. Shilov, Y.A. Rozhkova, L.N. Markova, M.A. Tashkinov, I.V. Vindokurov, V. V. Silberschmidt, Biocompatibility of 3D-printed PLA, PEEK and PETG: adhesion of bone marrow and peritoneal lavage cells, Polymers (Basel) 14 (19) (2022), https://doi.org/10.3390/polym14193958.

[93] M. Roskies, J.O. Jordan, D. Fang, et al., Improving PEEK bioactivity for craniofacial reconstruction using a 3D printed scaffold embedded with mesenchymal stem cells, J. Biomater. Appl. 31 (1) (2016) 132–139, https://doi.org/10.1177/0885328216638636/FORMAT/EPUB.

[94] H.V. Kruse, D.R. McKenzie, J.R. Clark, N. Suchowerska, Plasma ion implantation of 3D-printed PEEK creates optimal host conditions for bone ongrowth and mineralisation, Plasma Process. Polym. 18 (5) (2021), https://doi.org/10.1002/ppap.202000219.

[95] X. Liu, L. Huang, H. Zhang, et al., Facile amidogen bio-activation method can boost the soft tissue integration on 3D printed poly–ether–ether–ketone interface, Adv. Mater. Interfaces 8 (19) (2021), https://doi.org/10.1002/admi.202100547.

[96] B. Zhang, J. Leng, Z. Ouyang, et al., Superhydrophilic and topography-regulatable surface grafting on PEEK to improve cellular affinity, Biomater. Adv. 146 (2023), 213310, https://doi.org/10.1016/j.bioadv.2023.213310.

[97] T. Nishimura, Y. Ogino, Y. Ayukawa, K. Koyano, Influence of the wettability of different titanium surface topographies on initial cellular behavior, Dent. Mater. J. 37 (4) (2018) 650–658, https://doi.org/10.4012/dmj.2017-334.

[98] T. Ishizaki, N. Saito, O. Takai, Correlation of cell adhesive behaviors on superhydrophobic, superhydrophilic, and micropatterned superhydrophobic/superhydrophilic surfaces to their surface chemistry, Langmuir 26 (11) (2010) 8147–8154, https://doi.org/10.1021/la904447c.

[99] C.M. Han, E.J. Lee, H.E. Kim, et al., The electron beam deposition of titanium on polyetheretherketone (PEEK) and the resulting enhanced biological properties, Biomaterials 31 (13) (2010) 3465–3470, https://doi.org/10.1016/j.biomaterials.2009.12.030.